



Published in final edited form as:

Mol Psychiatry. 2017 August ; 22(8): 1140–1148. doi:10.1038/mp.2016.51.

Insulin Signaling Misregulation underlies Circadian and Cognitive Deficits in a *Drosophila* Fragile X Model

Rachel E. Monyak, B.A.¹, Danielle Emerson, B.A.¹, Brian P. Schoenfeld, B.A.^{1,2}, Xiangzhong Zheng, Ph.D.³, Daniel B. Chambers, B.A.⁴, Cory Rosenfelt, B.A.⁴, Steven Langer, B.A.⁴, Paul Hinchey, B.A.², Catherine H. Choi, M.D.^{2,5}, Thomas V. McDonald, M.D.², Francois V. Bolduc, M.D., Ph.D.⁴, Amita Sehgal, Ph.D.³, Sean M.J. McBride, M.D., Ph.D.^{6,*}, and Thomas A. Jongens, Ph.D.^{1,*}

¹Department of Genetics, Perelman School of Medicine at the University of Pennsylvania, Philadelphia, PA 19104-5158

²Section of Molecular Cardiology, Departments of Medicine and Molecular Pharmacology, Albert Einstein College of Medicine, Bronx, New York 10461

³Department of Neuroscience and Howard Hughes Medical Institute, Perelman School of Medicine at the University of Pennsylvania, Philadelphia, PA 19104-5158

⁴Department of Pediatric Neurology, Center for Neuroscience, University of Alberta, Edmonton, Canada AB T6G 2H7

⁵Department of Dermatology, Drexel University College of Medicine, 219 N. Broad Street, Philadelphia, PA, 19107

⁶Department of Psychiatry, Perelman School of Medicine at the University of Pennsylvania, Philadelphia, PA 19104-5158

Abstract

Fragile X syndrome (FXS) is an undertreated neurodevelopmental disorder characterized by low IQ and a wide range of other symptoms including disordered sleep and autism. Although FXS is the most prevalent inherited cause of intellectual disability, its mechanistic underpinnings are not well understood. Using *Drosophila* as a model of FXS, we showed that select expression of *dfmr1* in the insulin-producing cells (IPCs) of the brain was sufficient to restore normal circadian behavior and to rescue the memory deficits in the fragile X mutant fly. Examination of the insulin-signaling (IS) pathway revealed elevated levels of *Drosophila* insulin-like peptide 2 (Dilp2) in the IPCs and elevated IS in the *dfmr1* mutant brain. Consistent with a causal role for elevated IS in *dfmr1* mutant phenotypes, expression of *dfmr1* specifically in the IPCs reduced IS, and genetic reduction of the insulin pathway also led to amelioration of circadian and memory defects. Furthermore we showed that treatment with the FDA approved drug metformin also rescued

Users may view, print, copy, and download text and data-mine the content in such documents, for the purposes of academic research, subject always to the full Conditions of use: http://www.nature.com/authors/editorial_policies/license.html#terms

*To whom correspondence should be addressed: jongens@mail.med.upenn.edu and smjmcbride@gmail.com, phone: 215-573-9332, fax: 215-573-9411.

Conflict of Interest: The authors declare no conflicts of interest.

Supplementary information is available at *Molecular Psychiatry's* website.

memory. Finally, we showed that reduction of IS is required at different time points to rescue circadian behavior and memory. Our results indicate that insulin misregulation underlies the circadian and cognitive phenotypes displayed by the *Drosophila* fragile X model, and thus reveal a metabolic pathway that can be targeted by new and already approved drugs to treat fragile X patients.

Introduction

Fragile X Syndrome (FXS) is caused by loss of expression of FMR1, an RNA binding protein involved in the translation, stability and transport of up to 4% of human mRNAs (1, 2). FXS is the most commonly inherited form of intellectual disability and autism, and patients also suffer from attention deficit hyperactivity disorder, seizures, and disordered sleep (2-4). Loss of *FMR1* also results in noted neuro-anatomical defects, specifically an increased number of spines which are often elongated and immature (3, 4).

FXS is a life-long illness which is detrimental to both the patients and their caregivers (5, 6). A wide variety of drugs are used to treat the aggression, hyperactivity, anxiety and seizures associated with FXS, but no drugs are specifically approved for the treatment of the disease and those that are often used often have questionable efficacy (7). Although several promising drugs have recently been testing in clinical trials, they have failed to meet FDA approval (7), highlighting an urgent need to obtain drug targets and a more complete understanding of signaling pathways implicated in FXS pathogenesis to identify new targets for therapy.

To better understand disease pathogenesis, we use a *Drosophila* fragile X model, based on loss of *dfmr1* function, which displays several relevant phenotypes, including defects in the circadian output pathway, memory in the conditioned courtship and olfactory conditioning paradigms, social interaction (with peers and in naïve courtship), and neural development (8-12). Furthermore, signaling pathways found to be altered in the *dfmr1* mutant fly are often conserved in the mouse FXS model. Notably, the mGluR pathway has been shown to be misregulated in both mouse and fly models of FXS, and importantly, treatment with mGluR inhibitors rescues memory and other phenotypes in both *Drosophila* and mammalian models of the disease (10, 13). This strong conservation indicates the fly model is an extremely valuable tool to elucidate the underlying pathologies of FXS and test possible drug treatments.

In this study, we show that insulin signaling (IS) is increased in the brains of *dfmr1* mutants and that reducing IS either through the select expression of *dfmr1* in the insulin-producing cells (IPCs) or through genetic reduction of IS rescues both memory and circadian rhythmicity defects. We also demonstrate that rescue of the circadian defect requires reduction of IS during pupal development, whereas memory can be rescued by reducing IS in adults. Finally, we determine that treatment with the insulin-normalizing drug metformin improves memory in *dfmr1* mutants. Together, these findings reveal another signaling pathway involved in both memory and circadian behavior in FXS, and suggest a possible drug that might ameliorate cognitive defects.

Materials and Methods

Fly stocks and maintenance

Fly stocks were maintained on standard cornmeal-molasses medium. Fly Stocks containing *per-Gal4* (line 2), *tim-Gal4* (line 82), *clk8.0-Gal4*, *cry-Gal4*, *pdf-Gal4* are previously described (14-17). *Dilp2^R-Gal4* and *dilp2^W-Gal4*-containing stocks were obtained from Eric Rulifson and Peng Shen (18, 19). Fly strains containing the *dilp2* and *InR⁵⁵⁴⁵* mutations were obtained from Bloomington Stock Center (stock numbers 30881 and 11661) (20, 21). Fly stocks carrying the *UAS-DP110^{DN}* and *UAS-PTEN* transgenes were obtained from M. Birnbaum (22, 23). The *elav-Gal4* transgene was derived from Bloomington Stock number 8765. The *dfmr1³* allele and *WTrescue* are previously described in (9). The *Gal80^S* lines were derived from Bloomington Stock #7018. Flies used for the olfactory learning assay were outcrossed to *w1118(isoCJI)* flies. Flies used for temperature shift assays and metformin developmental studies were outcrossed to *w1118(iso31B)* flies.

Circadian Behavior Assay

Circadian analysis was conducted as described in (9). Rhythmicity was defined as a FFT value of 0.01 or more. Significance was determined using a Kruskal-Wallis test followed by a Dunn's post-test (GraphPad, InStat). Relative FFT = $\text{FFT}_{\text{experimental}}/\text{FFT}_{\text{wild-type}} * 100$.

For drug treatment, flies were raised on food containing 30 μ M or 100 μ M metformin or vehicle. Within 24 hours of eclosion, adult males were collected and maintained on food containing 1mM metformin or vehicle.

For temperature shift experiments, flies with *Gal80^S* were raised at 18°C. White 0-hour pupae or adults were collected and moved to 29°C for 2 days, then moved to 25°C to reduce deleterious effects caused by high temperature.

Short-term memory assay

The conditioned courtship assay was conducted as described in (10). For data not normal after transformation, the Mann-Whitney test was used to generate p-values (24). Statistics were performed using Statview 3.0 and Prism. Memory Index (MI) = $(\text{CI}_{\text{naive}} - \text{CI}_{\text{trained}})/\text{CI}_{\text{naive}}$ (25).

For drug treatment, flies were raised on food containing 30 μ M or 100 μ M metformin or vehicle. Adult male flies were collected within 4 hours of eclosion and placed on food containing 1mM or 5mM metformin or vehicle. One day before STM testing flies were moved to individual vials containing standard fly food.

For temperature shift assays, flies with *Gal80^S* were raised at 22°C, then moved to 27°C within 4 hours of eclosion. (22°C was used as the permissive temperature due to the deleterious effects of 18°C on courtship). All flies were moved to 25°C the night prior to testing and were tested at 25°C.

Western analysis

The heads of 3-7 day old flies were removed and placed on dry ice. Westerns were performed as described in (26). Primary antibodies used were: Anti- β -tubulin (Developmental Studies Hybridoma Bank, E7) 1:20,000, Anti-Akt (pan) (Cell Signaling Technologies, 4691) 1:5000, Anti-GFP (Aves Labs, GFP-1020) 1:2,500.

Immunofluorescence

Brain dissections and staining were performed as described in (26) then mounted in a 1:5 mixture of Prolong Gold (Invitrogen, P36930) and glycerol with 2% N-propyl gallate (Sigma, P3130). Primary antibodies used were: anti-dFMR1 (6A15) (Abcam, ab10299) 1:2000, anti-DE-cadherin (Developmental Studies Hybridoma Bank, DCAD2) 1:50, anti-GFP (Aves Labs, GFP-1020) 1:1500, anti-p-S473-Akt (D9E) (Cell Signaling Technologies, 4060) 1:800 (note that this antibody recognizes the S505 phosphorylation site in *Drosophila* which is analogous to the S473 phosphorylation site in mammals (27)), and anti-Dilp2, a gift from Eric Rulifson. Images were taken using a Leica TCS SP microscope with the settings kept constant throughout imaging. Leica LAS AF Lite software was used for quantification of confocal images. Significance was determined using an unpaired t-test with Welch's correction or Mann-Whitney test (GraphPad, InStat).

When quantifying Dilp2 staining, the average pixel intensity was recorded for 6 elliptical areas in the cytoplasm of 5 cells in each brain. When quantifying GFP-PH localization, images were taken of the posterior surface of the brain in the mushroom body calyx region because this area contains a large number of cell bodies. The ratio of the membrane fluorescence/cytoplasm fluorescence was determined for 20 cells in each hemisphere of the brain. When quantifying pAkt staining, images were taken of the posterior surface of the brain in the mushroom body calyx region. The average p-S505-Akt and DE-cadherin fluorescence of the cells in region was measured, then the p-S505-Akt fluorescence was normalized to that of DE-cadherin to control for staining differences between brains.

RNA isolation and quantitative PCR

Heads were homogenized in Tri-Reagent (Sigma) and RNA was isolated and purified using the RNeasy Mini Kit (Qiagen, 74104). cDNA was synthesized with Superscript III (Invitrogen, 18080-051) and Oligo dT primers. qPCR was performed using Brilliant III Ultra Fast Sybr Master Mix (Agilent Technologies, 600882) on the MxPro 3000 system (Agilent Technologies). *Dilp2* transcript levels were normalized to three reference genes (*SdhA*, *α Tub84B* and *14-3-3 ϵ*) by taking the geometric mean as described in (28). Samples consisted of 200 heads. *Dilp2* primers are described in (20) and *SdhA* primers are described in (29). The *α Tub84B* primers were: forward: 5'-CTTGTCGCGTGTGAAACACT-3' and reverse: 5'-AGCAGTAGAGCTCCCAGCAG-3' and the *14-3-3 ϵ* primers were: forward: 5'-GAGCGCGAGAACAATGTGTA-3' and reverse: 5'-ACGGTCAGCTCTACGTCCAT-3'. All primer concentrations were optimized to produce 100% amplification efficiency.

Pavlovian olfactory learning and memory

Full details of this assay are described in (12).

For drug treatment, flies were placed in vials overnight at 25°C and 70% humidity with Whatman filter paper containing 200 μ L of either 1mM metformin or vehicle and 5% sucrose.

For temperature shift experiments, flies were raised at 18°C, moved to 27°C after eclosion and incubated for 4 days prior to testing learning.

Results

Mapping studies indicate role for IPCs in circadian output

Previous studies of *dfmr1* mutants revealed that they display arrhythmic locomotor activity in free-running conditions due to a defect in the circadian output pathway (9, 30). To identify the mechanism through which *dfmr1* regulates circadian behavior, we utilized the binary Gal4/UAS system (31) to determine its spatial requirement for normal circadian rhythms. We first verified that *dfmr1* activity is required in the nervous system by restoring pan-neuronal *dfmr1* expression in an otherwise null mutant fly. We found that *dfmr1* mutants containing both the pan-neuronal driver, *elav-Gal4*, and *UAS-dfmr1* transgenes displayed significant improvement in free running behavior compared to mutant flies containing either *UAS-dfmr1* or *elav-Gal4* alone (Figure 1a, Supplementary Table 1). These results indicate that expression of *dfmr1* in the nervous system is sufficient to rescue the circadian defect observed in *dfmr1* null flies.

Circadian studies have defined a fly pacemaker circuit that consists of approximately 150 neurons (32). To determine if *dfmr1* activity within this circuit is sufficient to restore normal circadian behavior, we introduced several *Gal4* drivers that direct expression to a subset of or all clock cells into the *dfmr1* mutant background. First we used *pdf-Gal4* and *cry-Gal4* to express *dfmr1* in the ventral lateral neurons (LN_v), which have been shown to display morphological defects in the *dfmr1* mutants and are essential for maintenance of free-running rest:activity patterns (9, 14, 33-35). However expression of *dfmr1* in the LN_vs of *dfmr1* mutants did not increase the percentage of rhythmic flies or significantly raise relative FFT values, which measure the strength of circadian rhythmicity (Figure 1b, Supplementary Table 1). Similarly, using *per-Gal4* and *tim-Gal4* to more broadly direct *dfmr1* throughout the circadian clock circuit failed to discernibly rescue circadian behavior (Figure 1c, Supplementary Table 1).

We then explored the possibility that *dfmr1* activity was required outside the established circadian clock circuit by testing *Gal4* drivers that direct expression to neurons outside the defined clock circuit. Interestingly, we found that expression of *dfmr1* using two independent *dilp2-Gal4* drivers led to a significant rescue of rhythmicity that was comparable to the rescue obtained with *elav-Gal4* (Figure 1d, Supplementary Table 1, Supplementary Figure 1a). The *dilp2-Gal4* drivers direct expression to 14 insulin-producing neurons located in both hemispheres of the *pars intercerebralis* (P.I.) region of the brain (Supplementary Figure 1b), a neuroendocrine center that is important for circadian regulation in other insects and proposed to be important in *Drosophila* (16, 36). These neurons, termed the insulin-producing cells (IPCs), are the sole insulin-producing neurons in

the fly brain (18) (Supplementary Figure 1c). Our results indicate that providing *dfmr1* function to the IPCs is sufficient to rescue the circadian defect displayed by *dfmr1* mutants.

IS is elevated in *dfmr1* mutant brains

Given that expression of *dfmr1* in the IPCs rescues the circadian defect, we explored the possibility that IS was misregulated in *dfmr1* mutants. Examination of the levels of the major insulin-like peptide *Drosophila* insulin-like peptide 2 (*Dilp2*) consistently revealed significantly elevated *Dilp2* protein in the cell bodies and axons of *dfmr1* mutant versus control IPCs (Figures 2a and b, Supplementary Figure 2a). Conversely, *dilp2* mRNA levels are not increased in *dfmr1* mutant flies compared to controls, suggesting that *Dilp2* protein levels are increased by a post-transcriptional mechanism (Supplementary Figure 2b).

To determine how the altered expression levels of *Dilp2* in the IPCs impacts IS in the *dfmr1* mutant brain, we first examined PI3K activity using a ubiquitously expressed GFP-pleckstrin homology (PH) domain reporter. This reporter protein localizes to the plasma membrane upon stimulation of the insulin pathway as the concentration of phosphatidylinositol (3,4,5)-triphosphate is increased by activated PI3K (37). Although the GFP-PH reporter is seen broadly throughout the brain, we visualized and quantitated reporter protein localization in the cells on the posterior surface of the brain in the mushroom body calyx region because this area of the brain contains a large number of easily imaged cell bodies. We found that the GFP-PH reporter protein was more strongly localized to the plasma membrane in *dfmr1* mutant versus control brain neurons (Figures 2c and d), indicating that PI3K activity levels are elevated in the examined region of the *dfmr1* mutant brain. Subsequent examination of GFP-PH reporter protein expression by Western analysis revealed that reporter expression is similar in both *dfmr1* mutant and control heads (Supplementary Figures 3a and b). These results confirmed that the changes observed by immunofluorescence reflect alterations in PI3K activity rather than changes in reporter protein expression levels. We next examined Akt phosphorylation at S505, the site of its activation, using whole mount immunostaining and confocal analysis. With this method we observed a more pronounced concentration of p-S505-Akt at the plasma membrane in *dfmr1* mutant brains compared to controls (Supplementary Figures 3c and d). The increased concentration of p-S505-Akt seen in *dfmr1* mutants was significantly decreased by directed expression of *dfmr1* to the IPCs of *dfmr1* mutant brains (Figures 2e and f), indicating that the expression of *dfmr1* in these cells corrects the elevated IS in *dfmr1* mutant brains in a cell non-autonomous manner. Western analysis of total Akt expression in heads revealed that overall Akt expression remained constant, indicating that the increase in p-S505-Akt levels in *dfmr1* mutants is due to increased Akt activity rather than changes in Akt expression levels (Supplementary Figure 3e).

Reducing IS rescues circadian rhythmicity in *dfmr1* mutants

The studies described above demonstrated that expression of *dfmr1* specifically in the IPCs corrected IS in the mutants, suggesting that the circadian phenotype displayed by the *dfmr1* mutants could be rescued by reducing signaling through this pathway. To directly test the effect of reducing IS in *dfmr1* mutants, we performed four independent genetic manipulations in the *dfmr1* mutant background. We genetically reduced the gene dosage of

dilp2 and the insulin receptor (*InR*) by introducing a null allele of *dilp2* or a strong hypomorphic allele of *InR* into the *dfmr1* mutant background. We also genetically reduced PI3K activity by pan-neuronally expressing a dominant negative form of the 110kD catalytic subunit (*UAS-DP110^{DN}*) in the *dfmr1* mutant background using *elav-Gal4*. Finally, we elevated the expression of the Phosphatase and tensin homolog protein (PTEN), which antagonizes PI3K activity, using *UAS-PTEN* in combination with *elav-Gal4*. All four genetic manipulations led to statistically significant rescue of the free-running rhythm defect displayed by *dfmr1* mutants (Figures 3a to d, Supplementary Table 2). These results confirm that elevated IS contributes to the circadian phenotype displayed by *dfmr1* mutants.

Aberrant IS contributes to memory defects in *dfmr1* mutants

In mouse studies the PI3K-Akt-mTOR pathway has been found to be altered in the hippocampus of the *FMR1* KO mouse and linked to synaptic plasticity defects displayed by this FXS model (38, 39). To determine if increased IS is linked to the courtship conditioning-based short-term memory (STM) defect displayed by *dfmr1* mutants, we first determined if IPC-directed expression of *dfmr1* could rescue STM in *dfmr1* mutants. We observed restoration of STM in *dfmr1* mutants which expressed *dfmr1* in the IPCs, but not in *dfmr1* mutant controls (Figure 4a). These results indicate that normalization of the insulin-signaling pathway through expression of *dfmr1* in the IPCs restores STM in *dfmr1* mutants. To directly test if reduced IS corrects the STM defects, we tested STM in *dfmr1* mutants that carried one null allele of *dilp2*, or that had pan-neuronal expression of DP110^{DN} or PTEN. We found that STM was restored in *dfmr1* mutants by genetically reducing the gene dosage of *dilp2* (Figure 4b). Pan-neuronal expression of either DP110^{DN} or PTEN also restored STM, while the STM defect was not restored in *dfmr1* controls (Figures 4c and d). Interestingly, pan-neuronal expression of DP110^{DN} eliminated STM in wild-type flies even though it rescued STM in *dfmr1* mutants (Figure 4c), suggesting that any alteration in normal IS can negatively affect memory. In sum, these results indicate that enhanced IS contributes to the STM defect in *dfmr1* mutants.

Since normalization of IS restored STM in *dfmr1* mutants, we explored how alteration of IS affected defective immediate recall memory, hereafter referred to as learning, and long-term (1-day) memory (LTM) in the classical conditioning olfactory memory paradigm. We found that expression of *dfmr1* in the IPCs rescued both learning and LTM after spaced training in flies trained to associate a shock with an odor stimulus (Figures 4e and f). As expected, *dfmr1* mutant controls showed impaired learning and LTM (Figures 4e and f). Furthermore, genetic reduction of IS by pan-neuronal expression of DP110^{DN} also restored learning and LTM, while *dfmr1* mutant controls with either the *elav-Gal4* or *UAS-DP110^{DN}* transgenes alone did not exhibit improved learning or LTM (Figures 4g and h). These results indicate that enhanced IS also contributes to the defective olfactory-based memory seen in *dfmr1* mutant flies.

Metformin treatment ameliorates memory defects in *dfmr1* mutants

Given the misregulation of IS in *dfmr1* mutants, we explored treatment with metformin, a widely-used drug for type 2 diabetes that acts as an IS sensitizer. Several mechanisms have been suggested to explain the efficacy of metformin in the treatment of type 2 diabetes, but

we selected this drug because it is known to increase PTEN expression and AMPK activation, and to decrease TOR signaling (40-42). We found that *dfmr1* mutant flies reared on food containing metformin for 4-6 days after eclosion exhibited restored STM in the conditioned courtship memory paradigm in contrast to mutant flies fed food containing only vehicle (Figure 5a). We also tested classical olfactory conditioning memory in adult *dfmr1* mutant flies treated acutely with metformin overnight prior to training. We found that metformin treatment rescued both olfactory learning and protein synthesis-dependent LTM in *dfmr1* mutants (Figures 5b and c, Supplementary Figure 4a). We replicated previous results in which *dfmr1* mutant flies showed no defects in olfaction or shock sensitivity (12), and also observed that metformin did not exert its effect via enhanced olfaction or shock reactivity, confirming that metformin rescues cognitive rather than sensory defects (Supplementary Figure 4b and c). These results show that treatment with a drug known to target the IS pathway rescues several forms of memory in *dfmr1* mutant flies.

Following the result that acute metformin treatment rescued defects in both courtship-based and olfactory-based memory, we examined how metformin treatment during development and/or adulthood affected both memory and circadian behavior. While we were unable to rescue circadian rhythmicity with any combination of developmental and adulthood metformin treatment (Supplementary Figures 5a and b), we found that STM was amenable to rescue with several combinations of temporally-restricted metformin treatment (Supplementary Figures 5c and d). Intriguingly, we were able to rescue STM in the conditioned courtship paradigm with developmental treatment alone (Figures 5c and d). In contrast, developmental metformin treatment was unable to rescue learning or LTM in the olfactory conditioning paradigm (data not shown). The divergence in the timing of rescue of these two forms of memory may be due to differences in the inputs required for formation of these memories. Olfactory-based memory formation is solely dependent on an olfactory stimulus, while courtship-based memory involves a combination of olfactory, gustatory, visual and social inputs (43, 44). Since not all these inputs need to be present for courtship-based memory formation (45), we propose that some of these inputs may be rescued by developmental metformin treatment, while others may be rescued by physiological metformin treatment, thus allowing rescue of courtship-based memory to occur at several different time points.

Reduction of IS during the pupal period is required for normal circadian rhythmicity in *dfmr1* mutants

To more directly explore the temporal requirements of IS normalization for circadian rhythmicity, we used a temperature-sensitive Gal80 (*Gal80^{ts}*) to initiate IS reduction at different developmental stages. At its permissive temperature of 18°C, *Gal80^{ts}* prevents Gal4 function, while at its restrictive temperatures of 29°C, *Gal80^{ts}* function is abolished, allowing normal Gal4 activity (46). We used this system to test the effect of initiating IS reduction at the beginning of the pupal stage or within 24 hours of eclosion. Interestingly, we found that when IS was reduced using DP110^{DN}, the reduction had to occur during the pupal period to achieve rescue of circadian behavior (Supplementary Figure 6a and b). A similar result was observed when IS was reduced by PTEN overexpression, though comparison to one control did not reach significance (Supplementary Figure 6c and d).

These results suggest that normalization of IS during the pupal period is necessary for rescue of circadian behavior. This finding may also explain the inability of metformin treatment to rescue circadian behavior, as flies do not consume the metformin-treated food during the pupal period.

Since metformin treatment in adulthood alone rescued both olfactory-based and courtship-based memory, we used the Gal80^{ts} to test whether initiating reduction of IS in adulthood would also be sufficient to rescue memory in these assays. Adulthood-restricted reduction of IS using either pan-neuronal DP110^{DN} or PTEN expression rescued STM in the conditioned courtship paradigm (Supplementary Figure 6e). Similarly, adulthood reduction of IS by pan-neuronal DP110^{DN} expression was sufficient to rescue learning in the olfactory-based memory paradigm (Supplementary Figure 6f). Together, these results indicate that while physiological IS reduction is sufficient to rescue memory in the olfactory-based and courtship-based paradigms, reduction of IS during the pupal period is essential to rescue circadian behavior in *dfmr1* mutant flies. These findings suggest that the circadian and memory deficits seen in *dfmr1* mutant flies are ultimately caused by separate defects that are both affected by IS misregulation.

Discussion

FXS is serious illness affecting many individuals across the world (5). Because it is a major cause of autism and intellectual disability (3), revealing new signaling pathways disrupted in FXS will heighten our understanding of the signaling mechanisms underlying other forms of cognitive and social disabilities. Using an unbiased approach, we uncovered a connection between altered IS and FXS. Our findings raise several interesting questions about the mechanism by which dFMR1 influences IS, and whether altered IS contributes to behavior phenotypes in the mouse FXS models or to cognitive and/or sleep problems in human patients.

Although dFMR1 is expressed throughout the nervous system, we made the intriguing discovery that directing *dfmr1* expression to a small number of neurons could rescue two major behavioral phenotypes of the *dfmr1* mutant fly. These results raise the question of the mechanism by which dFMR1 functions in the IPCs to ensure normal IS. Although we are currently unable to pinpoint the precise mechanism, our results tell us that expression of *dfmr1* in the IPCs affects IS in a cell non-autonomous manner. Since dFMR1 is an RNA-binding protein which primarily represses the translation of its targets (1), one possibility is that dFMR1 directly binds to *dilp2* mRNA and represses its translation. In the absence of dFMR1, *dilp2* translation, and thus Dilp2 protein levels, would increase. This hypothesis is consistent with our findings that Dilp2 protein levels are increased in the IPCs while *dilp2* mRNA levels remain unchanged. A second possible mechanism is that dFMR1 acts more broadly within the IPCs to promote normal synaptic architecture and synapse formation. Importantly, loss of FMR1 in neurons is known to cause morphological defects in *Drosophila*, mice and humans (3, 4, 8, 9, 30, 34). Alterations in functional synapses between the IPCs and their neighboring neurons would likely have serious implications for IS, as the IPCs have been shown to receive inputs from multiple neurotransmitters and hormones, including corazonin, *Drosophila* tachykinin, GABA, octopamine, serotonin and sNPF (47).

Whatever the mechanism, our data suggest that *dfmr* expression in the IPCs is crucial for normal insulin release and IS in the brain.

The finding that *dfmr* has an important role in the IPCs raises the question of how this discovery translates to human patients. Curiously, the mammalian cells most analogous to the IPCs are the insulin-producing β -cells in the pancreas (18). FMR1 is expressed in β -cells, but its function in these cells is not established (48). However, although mammalian insulin-producing cells are not located in the brain, insulin and insulin-like growth factors have been ascribed many roles in the nervous system of both flies and mammals, including axon guidance, synaptogenesis, plasticity, progenitor cell proliferation and cellular metabolism (49-51). We show that IS in the brains of *dfmr* mutants is disrupted, and that this disruption contributes to behavioral phenotypes. These results suggest that exploring IS in other FXS models and in human patients may be revealing about disease pathogenesis. Indeed, data from the mouse model have identified elevated signaling in the PI3K-Akt-mTOR pathway that lies downstream of the insulin receptor (38, 39). Also, weight of *FMR1* KO mice is increased in early development relative to littermate controls, a finding that is also consistent with increased IS, at least in very young mutant pups (52). Interestingly, some observations of FXS patients hint that IS may be abnormal. A subgroup of patients exhibits a distinctive obese phenotype (53). Furthermore, a more recent study identified markers of elevated IS in the blood and brains of FXS patients (54). These observations could indicate that elevated IS is a conserved characteristic in the mouse FXS model and possibly FXS patients.

We found that reducing elevated IS in *dfmr* mutants ameliorates both the circadian and memory defects, suggesting that elevated IS contributes to these defects. Although no role for IS in circadian behavior has yet been established, we identified the pupal stage as a critical time period during which insulin signaling must be normalized to stimulate rhythmic circadian activity in adulthood. The pupal stage is a period of massive neuronal reorganization and since IS also has an important role in neural development (49), aberrant IS could result in improper reorganization of the circadian output circuit during metamorphosis. Interestingly, several studies hint at roles for IS in circadian behavior. Changes in IS affect sleep duration in older flies (55), which could also affect rhythmicity. Also, there are established interactions between IS and ecdysone signaling, which is already known to influence circadian rhythmicity (56-60). However, further experiments will be needed to establish the mechanisms by which alterations in IS affect circadian behavior.

Our findings also indicate that properly modulated IS is important for normal memory in *dfmr* mutants. Our discovery of the drug metformin as an enhancer of two forms of memory in *dfmr* mutant flies may provide some clues as to the mechanism of IS action on memory. The identification of metformin is particularly exciting because as a FDA approved drug, it could be used immediately in patients. However, although metformin is known to affect the IS pathway, its mechanism of action is currently unknown. Previous studies have shown that metformin raises pAMPK levels, which has the effect of reducing IS downstream of the TOR pathway (61). It should be noted, however, that metformin also acts through other pathways, including through cAMP and mitochondrial complex I (62, 63). Currently we can only speculate as to which pathways metformin targets to improve memory in *dfmr*

mutant flies, but further pursuit of this question will be important to understanding the mechanism by which memory is disrupted in FXS.

Here we show that normal IS is disrupted in *dfmr1* mutant flies, and that normalization of IS through genetic or pharmacological means is able to rescue circadian behavior and memory. Clearly further investigation will help unravel the connection between IS, memory and circadian behavior, and establish how metformin affects memory in *dfmr1* mutants. Exploration of these results in the mouse fragile X model and fragile X patients will be essential, as such investigations may lead to novel treatments for FXS and other disorders.

Supplementary Material

Refer to Web version on PubMed Central for supplementary material.

Acknowledgments

This work was supported by the FRAXA Research Foundation with grants to SMJM, CC, TAJ, and by the National Institutes of Health (NIH) Grant GM086902 to TAJ. The United States Department of Defense Autism Grant AR1101189 and Autism Speaks Grant AS2087 provided grant support for TAJ and SMJM. The Albert Einstein College of Medicine of Yeshiva University MSTP grant funded SMJM. SMJM was also supported by a University of Pennsylvania R25 MH060490 (Clinical Research Scholars Program in Psychiatry) and by the Training Program in Neuropsychopharmacology at the University of Pennsylvania T32 MH1465. RM was supported by a training grant from the NIH (T32 HD 7516-14) and XZ was supported by a NARSAD Young Investigator Award. CC was supported by the Dermatology Chairman's fund grant of Drexel University College of Medicine. FB was supported by grants from the Canadian Institute Health Research, Canadian Child Health Clinician Scientist Program and the Women and Children Health Research Institute. Experiments were performed by RM, DE, BS, XZ, DC, PH, TM, CC, FB, CR, SL, SMJM and TAJ. Experiments were designed by TAJ, RM, SMJM, FB and AS. The paper was written by RM and TAJ. The paper was edited by RM, DE, XZ, FB, AS, SMJM and TAJ. Figures were prepared by RM, DE and DC.

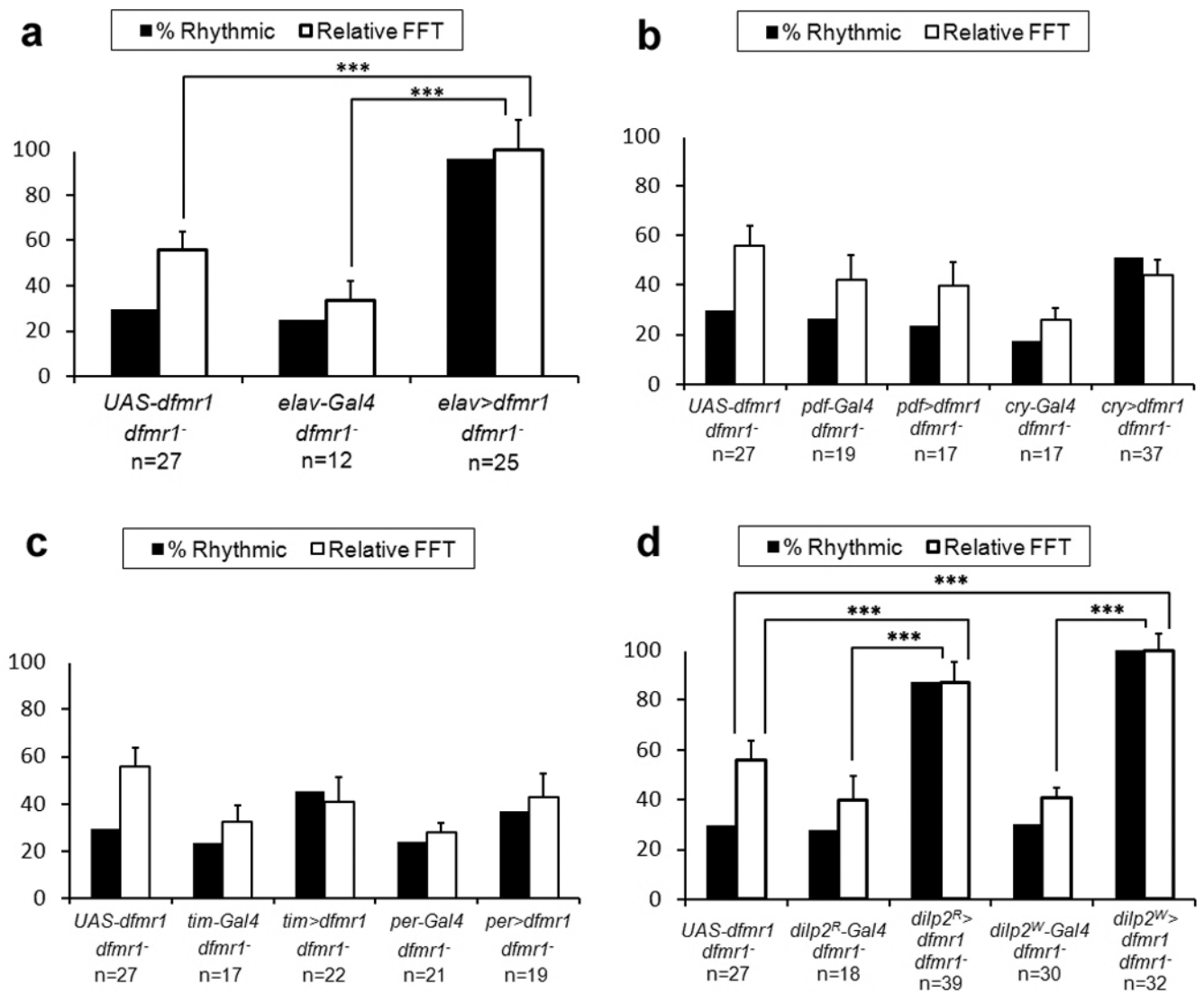
References

1. Santoro MR, Bray SM, Warren ST. Molecular mechanisms of fragile X syndrome: a twenty-year perspective. *Annual review of pathology*. 2012; 7:219–45.
2. Dolen G, Carpenter RL, Ocain TD, Bear MF. Mechanism-based approaches to treating fragile X. *Pharmacology & therapeutics*. 2010; 127(1):78–93. [PubMed: 20303363]
3. Jacquemont S, Hagerman RJ, Hagerman PJ, Leehey MA. Fragile-X syndrome and fragile X-associated tremor/ataxia syndrome: two faces of FMR1. *Lancet neurology*. 2007; 6(1):45–55. [PubMed: 17166801]
4. O'Donnell WT, Warren ST. A decade of molecular studies of fragile X syndrome. *Annual review of neuroscience*. 2002; 25:315–38.
5. Turk J. Fragile X syndrome: lifespan developmental implications for those without as well as with intellectual disability. *Current opinion in psychiatry*. 2011; 24(5):387–97. [PubMed: 21825875]
6. Cross J, Yang JC, Johnson FR, Quiroz J, Dunn J, Raspa M, et al. Caregiver Preferences for the Treatment of Males with Fragile X Syndrome. *Journal of developmental and behavioral pediatrics* : JDBP. 2016; 37(1):71–9. [PubMed: 26595147]
7. Schaefer TL, Davenport MH, Erickson CA. Emerging pharmacologic treatment options for fragile X syndrome. *The application of clinical genetics*. 2015; 8:75–93. [PubMed: 25897255]
8. Zhang YQ, Bailey AM, Matthies HJ, Renden RB, Smith MA, Speese SD, et al. Drosophila fragile X-related gene regulates the MAP1B homolog Futsch to control synaptic structure and function. *Cell*. 2001; 107(5):591–603. [PubMed: 11733059]
9. Dockendorff TC, Su HS, McBride SM, Yang Z, Choi CH, Siwicki KK, et al. Drosophila lacking *dfmr1* activity show defects in circadian output and fail to maintain courtship interest. *Neuron*. 2002; 34(6):973–84. [PubMed: 12086644]

10. McBride SM, Choi CH, Wang Y, Liebelt D, Braunstein E, Ferreiro D, et al. Pharmacological rescue of synaptic plasticity, courtship behavior, and mushroom body defects in a *Drosophila* model of fragile X syndrome. *Neuron*. 2005; 45(5):753–64. [PubMed: 15748850]
11. Bolduc FV, Valente D, Nguyen AT, Mitra PP, Tully T. An assay for social interaction in *Drosophila* Fragile X mutants. *Fly*. 2010; 4(3):216–25. [PubMed: 20519966]
12. Bolduc FV, Bell K, Cox H, Broadie KS, Tully T. Excess protein synthesis in *Drosophila* fragile X mutants impairs long-term memory. *Nature neuroscience*. 2008; 11(10):1143–5. [PubMed: 18776892]
13. Michalon A, Sidorov M, Ballard TM, Ozmen L, Spooren W, Wettstein JG, et al. Chronic pharmacological mGlu5 inhibition corrects fragile X in adult mice. *Neuron*. 2012; 74(1):49–56. [PubMed: 22500629]
14. Renn SC, Park JH, Rosbash M, Hall JC, Taghert PH. A pdf neuropeptide gene mutation and ablation of PDF neurons each cause severe abnormalities of behavioral circadian rhythms in *Drosophila*. *Cell*. 1999; 99(7):791–802. [PubMed: 10619432]
15. Emery P, Stanewsky R, Helfrich-Forster C, Emery-Le M, Hall JC, Rosbash M. *Drosophila* CRY is a deep brain circadian photoreceptor. *Neuron*. 2000; 26(2):493–504. [PubMed: 10839367]
16. Kaneko M, Hall JC. Neuroanatomy of cells expressing clock genes in *Drosophila*: transgenic manipulation of the period and timeless genes to mark the perikarya of circadian pacemaker neurons and their projections. *J Comp Neurol*. 2000; 422(1):66–94. [PubMed: 10842219]
17. Glossop NR, Houl JH, Zheng H, Ng FS, Dudek SM, Hardin PE. VRILLE feeds back to control circadian transcription of Clock in the *Drosophila* circadian oscillator. *Neuron*. 2003; 37(2):249–61. [PubMed: 12546820]
18. Rulifson EJ, Kim SK, Nusse R. Ablation of insulin-producing neurons in flies: growth and diabetic phenotypes. *Science*. 2002; 296(5570):1118–20. [PubMed: 12004130]
19. Wu Q, Zhang Y, Xu J, Shen P. Regulation of hunger-driven behaviors by neural ribosomal S6 kinase in *Drosophila*. *Proceedings of the National Academy of Sciences of the United States of America*. 2005; 102(37):13289–94. [PubMed: 16150727]
20. Gronke S, Clarke DF, Broughton S, Andrews TD, Partridge L. Molecular evolution and functional characterization of *Drosophila* insulin-like peptides. *PLoS genetics*. 2010; 6(2):e1000857. [PubMed: 20195512]
21. Fernandez R, Tabarini D, Azpiazu N, Frasch M, Schlessinger J. The *Drosophila* insulin receptor homolog: a gene essential for embryonic development encodes two receptor isoforms with different signaling potential. *The EMBO journal*. 1995; 14(14):3373–84. [PubMed: 7628438]
22. Leever SJ, Weinkove D, MacDougall LK, Hafen E, Waterfield MD. The *Drosophila* phosphoinositide 3-kinase Dp110 promotes cell growth. *The EMBO journal*. 1996; 15(23):6584–94. [PubMed: 8978685]
23. Huang H, Potter CJ, Tao W, Li DM, Brogiolo W, Hafen E, et al. PTEN affects cell size, cell proliferation and apoptosis during *Drosophila* eye development. *Development*. 1999; 126(23):5365–72. [PubMed: 10556061]
24. Siegel S. *Nonparametric Statistics*. *Am Stat*. 1957; 11(3):13–9.
25. Keleman K, Kruttner S, Alenius M, Dickson BJ. Function of the *Drosophila* CPEB protein Orb2 in long-term courtship memory. *Nature neuroscience*. 2007; 10(12):1587–93. [PubMed: 17965711]
26. Pepper AS, Beerman RW, Bhogal B, Jongens TA. Argonaute2 suppresses *Drosophila* fragile X expression preventing neurogenesis and oogenesis defects. *PloS one*. 2009; 4(10):e7618. [PubMed: 19888420]
27. Pinal N, Goberdhan DC, Collinson L, Fujita Y, Cox IM, Wilson C, et al. Regulated and polarized PtdIns(3,4,5)P3 accumulation is essential for apical membrane morphogenesis in photoreceptor epithelial cells. *Current biology : CB*. 2006; 16(2):140–9. [PubMed: 16431366]
28. Vandesompele J, De Preter K, Pattyn F, Poppe B, Van Roy N, De Paepe A, et al. Accurate normalization of real-time quantitative RT-PCR data by geometric averaging of multiple internal control genes. *Genome biology*. 2002; 3(7) RESEARCH0034.
29. Ling D, Salvaterra PM. Robust RT-qPCR data normalization: validation and selection of internal reference genes during post-experimental data analysis. *PloS one*. 2011; 6(3):e17762. [PubMed: 21423626]

30. Morales J, Hiesinger PR, Schroeder AJ, Kume K, Verstreken P, Jackson FR, et al. Drosophila fragile X protein, DFXR, regulates neuronal morphology and function in the brain. *Neuron*. 2002; 34(6):961–72. [PubMed: 12086643]
31. Brand AH, Perrimon N. Targeted gene expression as a means of altering cell fates and generating dominant phenotypes. *Development*. 1993; 118(2):401–15. [PubMed: 8223268]
32. Nitabach MN, Taghert PH. Organization of the Drosophila circadian control circuit. *Current biology : CB*. 2008; 18(2):R84–93. [PubMed: 18211849]
33. Helfrich-Forster C, Homberg U. Pigment-dispersing hormone-immunoreactive neurons in the nervous system of wild-type Drosophila melanogaster and of several mutants with altered circadian rhythmicity. *J Comp Neurol*. 1993; 337(2):177–90. [PubMed: 8276996]
34. Reeve SP, Bassetto L, Genova GK, Kleyner Y, Leyssen M, Jackson FR, et al. The Drosophila fragile X mental retardation protein controls actin dynamics by directly regulating profilin in the brain. *Current biology : CB*. 2005; 15(12):1156–63. [PubMed: 15964283]
35. Helfrich-Forster C. Robust circadian rhythmicity of Drosophila melanogaster requires the presence of lateral neurons: a brain-behavioral study of disconnected mutants. *Journal of comparative physiology A, Sensory, neural, and behavioral physiology*. 1998; 182(4):435–53.
36. Helfrich-Forster C, Stengl M, Homberg U. Organization of the circadian system in insects. *Chronobiology international*. 1998; 15(6):567–94. [PubMed: 9844747]
37. Britton JS, Lockwood WK, Li L, Cohen SM, Edgar BA. Drosophila's insulin/PI3-kinase pathway coordinates cellular metabolism with nutritional conditions. *Developmental cell*. 2002; 2(2):239–49. [PubMed: 11832249]
38. Sharma A, Hoeffler CA, Takayasu Y, Miyawaki T, McBride SM, Klann E, et al. Dysregulation of mTOR signaling in fragile X syndrome. *The Journal of neuroscience : the official journal of the Society for Neuroscience*. 2010; 30(2):694–702. [PubMed: 20071534]
39. Gross C, Nakamoto M, Yao X, Chan CB, Yim SY, Ye K, et al. Excess phosphoinositide 3-kinase subunit synthesis and activity as a novel therapeutic target in fragile X syndrome. *The Journal of neuroscience : the official journal of the Society for Neuroscience*. 2010; 30(32):10624–38. [PubMed: 20702695]
40. Kim SA, Choi HC. Metformin inhibits inflammatory response via AMPK-PTEN pathway in vascular smooth muscle cells. *Biochemical and biophysical research communications*. 2012; 425(4):866–72. [PubMed: 22898050]
41. Zhou G, Myers R, Li Y, Chen Y, Fenyk-Melody J, et al. Role of AMP-activated protein kinase in mechanism of metformin action. *The Journal of clinical investigation*. 2001; 108(8):1167–74. [PubMed: 11602624]
42. Lee JH, Budanov AV, Park EJ, Birse R, Kim TE, Perkins GA, et al. Sestrin as a feedback inhibitor of TOR that prevents age-related pathologies. *Science*. 2010; 327(5970):1223–8. [PubMed: 20203043]
43. Davis RL. Olfactory memory formation in Drosophila: from molecular to systems neuroscience. *Annual review of neuroscience*. 2005; 28:275–302.
44. Griffith LC, Ejima A. Multimodal sensory integration of courtship stimulating cues in Drosophila melanogaster. *Annals of the New York Academy of Sciences*. 2009; 1170:394–8. [PubMed: 19686165]
45. Joiner MI A, Griffith LC. CaM kinase II and visual input modulate memory formation in the neuronal circuit controlling courtship conditioning. *The Journal of neuroscience : the official journal of the Society for Neuroscience*. 1997; 17(23):9384–91. [PubMed: 9364084]
46. McGuire SE, Le PT, Osborn AJ, Matsumoto K, Davis RL. Spatiotemporal rescue of memory dysfunction in Drosophila. *Science*. 2003; 302(5651):1765–8. [PubMed: 14657498]
47. Nassel DR, Kubrak OI, Liu Y, Luo J, Lushchak OV. Factors that regulate insulin producing cells and their output in Drosophila. *Frontiers in physiology*. 2013; 4:252. [PubMed: 24062693]
48. Milochau A, Lagree V, Benassy MN, Chaignepain S, Papin J, Garcia-Arcos I, et al. Synaptotagmin 11 interacts with components of the RNA-induced silencing complex RISC in clonal pancreatic beta-cells. *FEBS letters*. 2014; 588(14):2217–22. [PubMed: 24882364]
49. Fernandez AM, Torres-Aleman I. The many faces of insulin-like peptide signalling in the brain. *Nature reviews Neuroscience*. 2012; 13(4):225–39. [PubMed: 22430016]

50. Song J, Wu L, Chen Z, Kohanski RA, Pick L. Axons guided by insulin receptor in *Drosophila* visual system. *Science*. 2003; 300(5618):502–5. [PubMed: 12702880]
51. Callan MA, Clements N, Ahrendt N, Zarnescu DC. Fragile X Protein is required for inhibition of insulin signaling and regulates glial-dependent neuroblast reactivation in the developing brain. *Brain research*. 2012; 1462:151–61. [PubMed: 22513101]
52. Dolen G, Osterweil E, Rao BS, Smith GB, Auerbach BD, Chattarji S, et al. Correction of fragile X syndrome in mice. *Neuron*. 2007; 56(6):955–62. [PubMed: 18093519]
53. Nowicki ST, Tassone F, Ono MY, Ferranti J, Croquette MF, Goodlin-Jones B, et al. The Prader-Willi phenotype of fragile X syndrome. *Journal of developmental and behavioral pediatrics : JDBP*. 2007; 28(2):133–8. [PubMed: 17435464]
54. Hoeffler CA, Sanchez E, Hagerman RJ, Mu Y, Nguyen DV, Wong H, et al. Altered mTOR signaling and enhanced CYFIP2 expression levels in subjects with fragile X syndrome. *Genes, brain, and behavior*. 2012; 11(3):332–41.
55. Yurgel ME, Masek P, DiAngelo J, Keene AC. Genetic dissection of sleep-metabolism interactions in the fruit fly. *Journal of comparative physiology A, Neuroethology, sensory, neural, and behavioral physiology*. 2015; 201(9):869–77.
56. Itoh TQ, Tanimura T, Matsumoto A. Membrane-bound transporter controls the circadian transcription of clock genes in *Drosophila*. *Genes to cells : devoted to molecular & cellular mechanisms*. 2011; 16(12):1159–67. [PubMed: 22077638]
57. Colombani J, Bianchini L, Layalle S, Pondeville E, Dauphin-Villemant C, Antoniewski C, et al. Antagonistic actions of ecdysone and insulins determine final size in *Drosophila*. *Science*. 2005; 310(5748):667–70. [PubMed: 16179433]
58. Okamoto N, Yamanaka N, Yagi Y, Nishida Y, Kataoka H, O'Connor MB, et al. A fat body-derived IGF-like peptide regulates postfeeding growth in *Drosophila*. *Dev Cell*. 2009; 17(6):885–91. [PubMed: 20059957]
59. Slaidina M, Delanoue R, Gronke S, Partridge L, Leopold P. A *Drosophila* insulin-like peptide promotes growth during nonfeeding states. *Dev Cell*. 2009; 17(6):874–84. [PubMed: 20059956]
60. Kumar S, Chen D, Jang C, Nall A, Zheng X, Sehgal A. An ecdysone-responsive nuclear receptor regulates circadian rhythms in *Drosophila*. *Nature communications*. 2014; 5:5697.
61. Slack C, Foley A, Partridge L. Activation of AMPK by the putative dietary restriction mimetic metformin is insufficient to extend lifespan in *Drosophila*. *PloS one*. 2012; 7(10):e47699. [PubMed: 23077661]
62. Miller RA, Chu Q, Xie J, Foretz M, Viollet B, Birnbaum MJ. Biguanides suppress hepatic glucagon signalling by decreasing production of cyclic AMP. *Nature*. 2013; 494(7436):256–60. [PubMed: 23292513]
63. Hur KY, Lee MS. New mechanisms of metformin action: Focusing on mitochondria and the gut. *Journal of diabetes investigation*. 2015; 6(6):600–9. [PubMed: 26543531]

**Figure 1.**

Expression of dFMR1 in the IPCs of the brain rescues defects in circadian behavior. **(a to d)**

Panels show the percent rhythmic (black) and relative FFT values (white) for genetic combinations testing the spatial requirement of dFMR1 expression in *dfmr1* mutants for normal circadian behavior. Relative FFT represents how the average FFT of the depicted genotype compares to the average FFT of a wild-type control. **(a)** *Dfmr1* mutants expressing *dfmr1* *pan-neuronally* display an increased percentage of rhythmic flies and more robust circadian rhythmicity than *dfmr1* mutants with either transgene alone, $p < 0.001$. **(b)** Circadian behavior of *dfmr1* mutants with both *pdf-Gal4* or *cry-Gal4* and *UAS-dfmr1* is not significantly different from *dfmr1* mutants with any of the relevant transgenes alone. **(c)** Circadian behavior of *dfmr1* mutants with *tim-Gal4* or *per-Gal4* and *UAS-dfmr1* is not significantly improved compared to *dfmr1* mutants with any of the relevant transgenes alone. **(d)** Circadian behavior of *dfmr1* mutants with both *dilp2^R-Gal4* or *dilp2^W-Gal4* and *UAS-dfmr1* is significantly improved relative to *dfmr1* mutants with any of the relevant transgenes

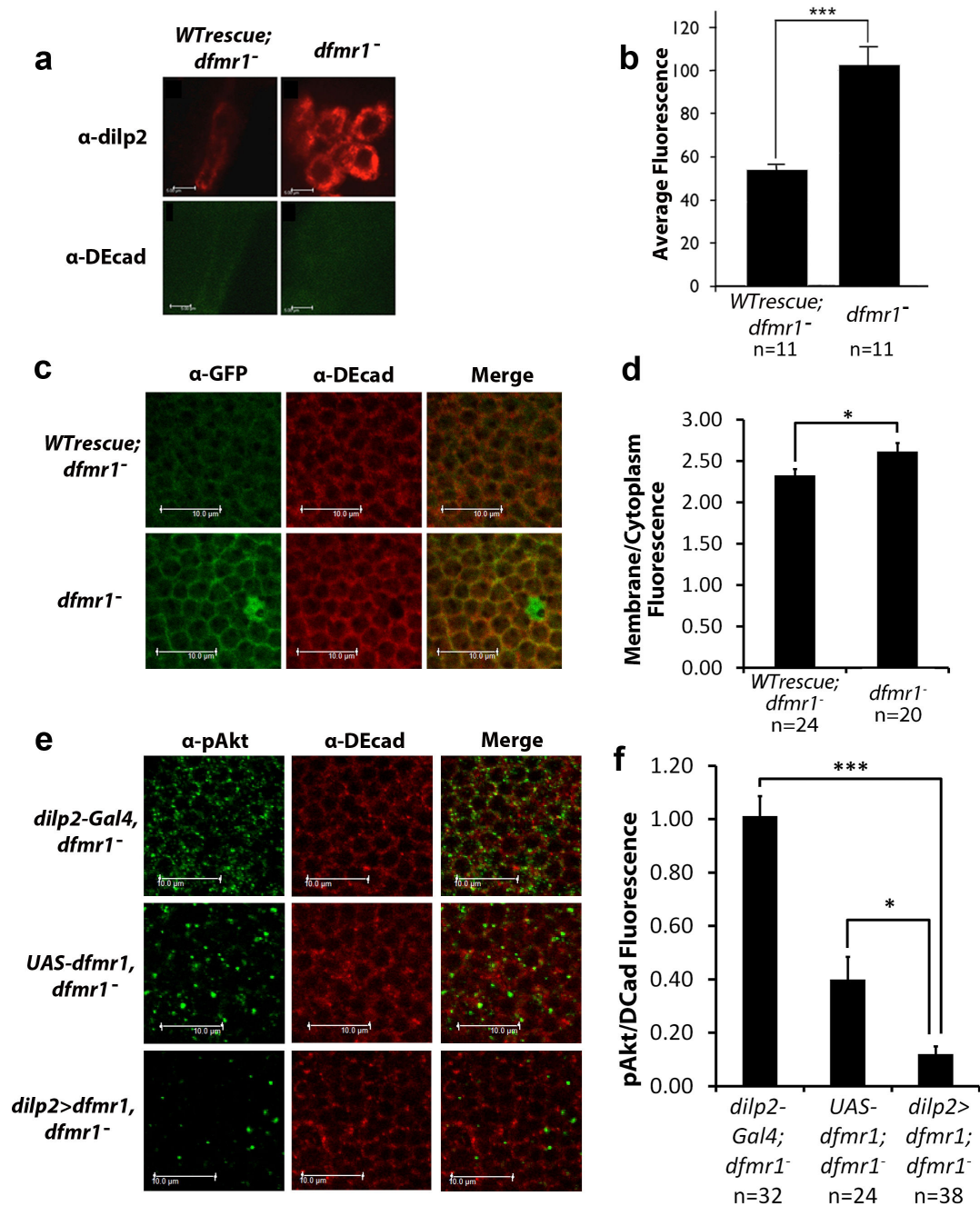
alone, $p < 0.001$. Statistically significant levels of rescue are denoted with asterisks (* $p < 0.05$, ** $p < 0.01$, *** $p < 0.001$). Error bars represent s.e.m.

Author Manuscript

Author Manuscript

Author Manuscript

Author Manuscript

**Figure 2.**

The IS pathway is upregulated in *dfmr1* mutant brains. **(a)** Dilp2 protein levels in the IPC cell bodies of *dfmr1* mutant brains are higher than in controls (*dfmr1* mutants containing a *WTrescue* transgene which expresses *dfmr1* at wild-type levels). DE-cadherin was used as a staining control. **(b)** Quantification reveals Dilp2 is significantly increased in *dfmr1* mutants, $p < 0.001$. **(c)** The GFP-PH reporter is more localized to the membrane in the cells of *dfmr1* mutant than in controls. Brains were imaged on their posterior side in the mushroom body calyx region. **(d)** Quantification of reporter distribution shown as a ratio of membrane/

cytoplasm fluorescence. *Dfmr1* mutants show a significantly higher ratio, $p < 0.05$. The membrane/fluorescence ratio was also calculated for the DE-cadherin staining control and was found to be the same in both genotypes (not shown). (e) A notable decrease in p-S505-Akt levels is observed in *dfmr1* mutants that have *dfmr1* expressed in the IPCs. (f) Quantification of p-S505-Akt fluorescence reveals that *dfmr1* mutants expressing *dfmr1* in the IPCs show significantly lower p-S505-Akt fluorescence than either *dfmr1* mutant control with the driver or UAS-construct alone, $p < 0.001$ and $p < 0.05$. p-S505-Akt fluorescence was normalized to DE-cadherin fluorescence. All images in this figure are representative of quantification.

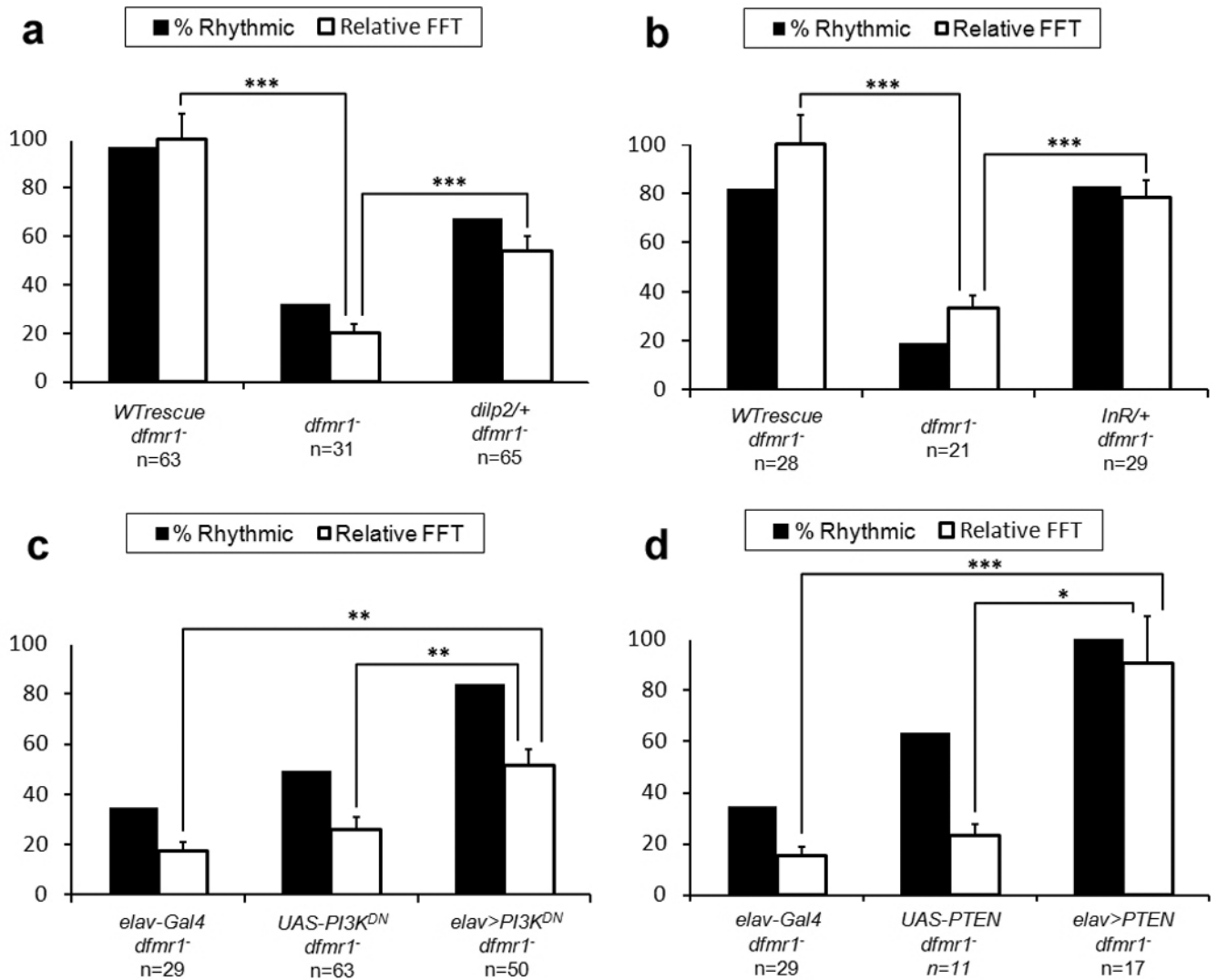


Figure 3.

Genetic reduction of the insulin pathway rescues the circadian defect observed in *dfmr1* mutants. **(a to d)** Panels show the percentage of rhythmic flies (black) and relative FFT values (white) for genetic combinations testing the effect of reducing IS in *dfmr1* mutants on circadian behavior. **(a)** Circadian behavior (as indicated by increased percentage of rhythmic flies and increased relative FFT) of *dfmr1* mutants with the *WTrescue* transgene or with one copy of a null allele of *dilp2* (*dilp2/+; dfmr1*) is significantly improved relative to *dfmr1* mutant controls, $p < 0.001$. **(b)** Circadian behavior of *dfmr1* mutants with the *WTrescue* transgene or with one copy of a mutant allele of the insulin receptor (*InR/+; dfmr1*) is significantly improved relative to *dfmr1* mutant controls, $p < 0.001$. **(c)** Circadian behavior of *dfmr1* mutants with both *elav-Gal4* and *UAS-DP110^{DN}* (*elav>DP110^{DN}; dfmr1*) is significantly improved relative to *dfmr1* mutants with either transgene alone (*elav-Gal4; dfmr1*) and (*UAS-DP110^{DN}; dfmr1*), $p < 0.01$. **(d)** Circadian behavior of *dfmr1* mutants with both *elav-Gal4* and *UAS-PTEN* (*elav>PTEN; dfmr1*) is significantly improved relative to *dfmr1* mutants with either transgene alone (*elav-Gal4; dfmr1*) and (*UAS-PTEN; dfmr1*),

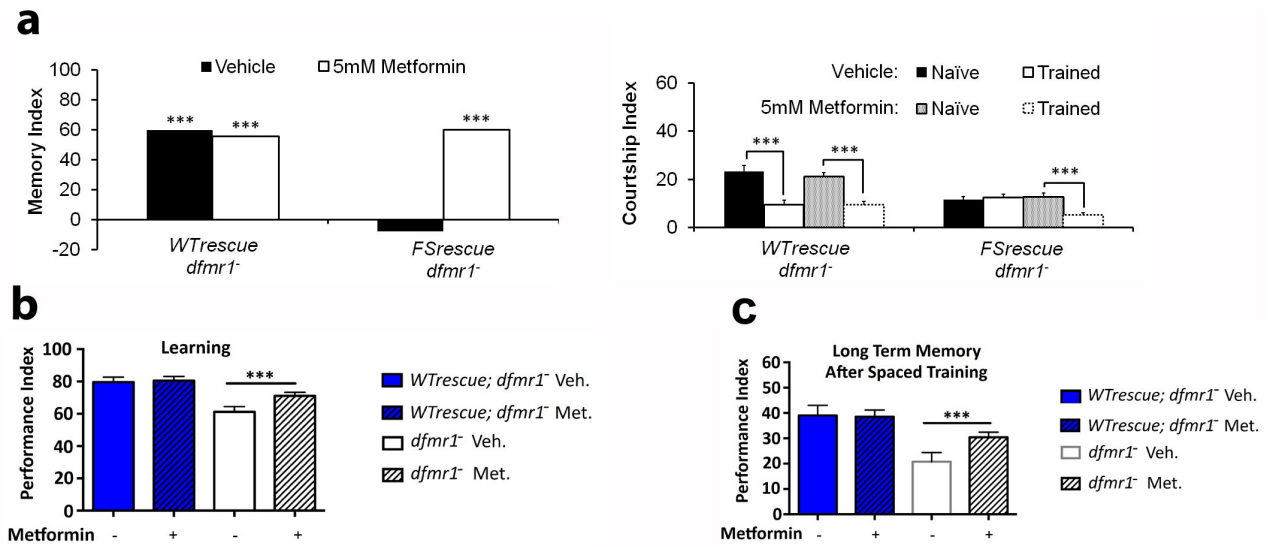
$p < 0.001$ and $p < 0.05$ respectively. Significance denoted as described in Fig. 1. Error bars represent s.e.m.

Author Manuscript

Author Manuscript

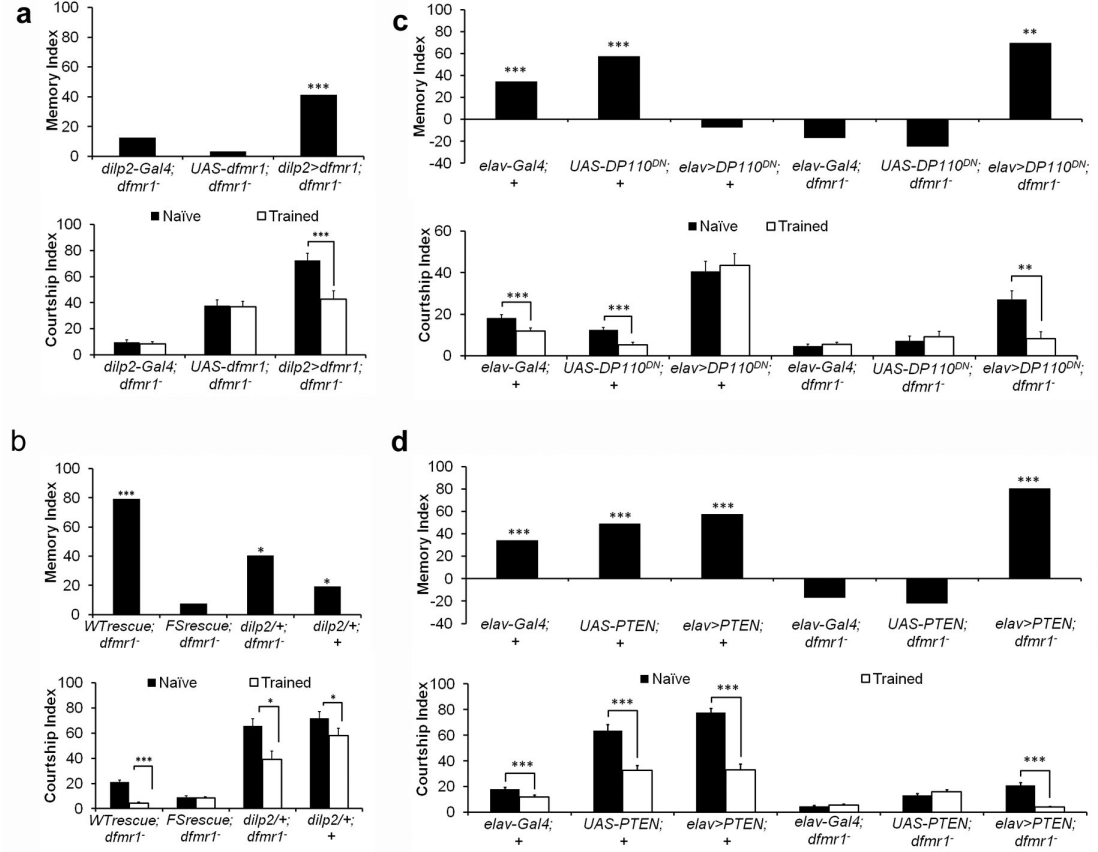
Author Manuscript

Author Manuscript

**Figure 4.**

Expression of dFMR1 in the IPCs and genetic reduction of IS rescue memory in *dfmr1* mutants. **(a to d)** STM in the courtship paradigm is presented as a memory index (left) which conveys the difference between the CIs of trained and untrained flies in a single values, and as separate CIs (right). **(a)** Expression of *dfmr1* in the IPCs of *dfmr1* mutants rescues STM, $p < 0.0001$, $N = 16-20$ **(b)** STM is rescued by reduction of *dilp2* in *dfmr1* mutants, $p < 0.05$. *FSrescue* represents a frame-shifted version of the *dfmr1* open reading frame. $N = 25-31$. **(c)** STM is rescued by pan-neural expression of DP110^{DN}, $p < 0.01$. $N = 22-91$ or **(d)** PTEN, $p < 0.001$. $N = 28-91$. **(e to h)** Performance index (PI) represents the percent of flies which avoid the shock-conditioned odor. **(e)** *Dfmr1* mutants expressing dFMR1 within the IPCs show rescue of learning, ($N = 4$, $p = 0.0016$) and **(f)** memory ($N = 8$, $p = 0.0002$). **(g)** *Dfmr1* mutants expressing DP110^{DN} pan-neuronally show rescue of learning ($N = 4$, $p = 0.0235$) and **(h)** memory, ($N = 8$, $p = 0.0005$). Graphs depict mean \pm s.e.m.

Courtship-based memory:



Olfactory-based memory:

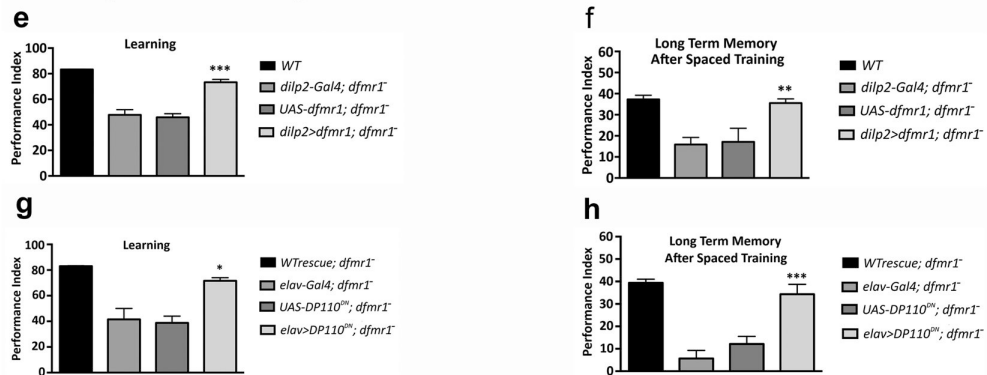


Figure 5.

Metformin treatment rescues memory in *dfmr1* mutants. (a) Metformin treatment restores STM to *dfmr1* mutants, $p < .001$ $N=36-86$. (b) Metformin improves learning ($p < 0.0001$). ($N=6$) and (c) memory in *dfmr1* mutants. ($N=8$, $p < 0.00018$). Graphs depict mean \pm s.e.m.